Observing upper troposphere–lower stratosphere climate with radio occultation data from the CHAMP satellite

Ulrich Foelsche · Michael Borsche · Andrea K. Steiner · Andreas Gobiet ·
Barbara Pirscher · Gottfried Kirchengast · Jens Wickert · Torsten Schmidt

Abstract High quality observations of the atmosphere are particularly required for monitoring global climate change. Radio occultation (RO) data, using Global Navigation Satellite System (GNSS) signals, are well suited for this challenge. The special climate utility of RO data arises from their long-term stability due to their self-calibrated nature. The German research satellite CHAllenging Mini-satellite Payload for geoscientific research (CHAMP) continuously records RO profiles since August 2001 providing the first opportunity to create RO based climatologies for a multi-year period of more than 5 years. A period of missing CHAMP data from July 3, 2006 to August 8, 2006 can be bridged with RO data from the GRACE satellite (Gravity Recovery and Climate Experiment). We have built seasonal and zonal mean climatologies of atmospheric (dry) temperature, microwave refractivity, geopotential height and pressure with 10° latitudinal resolution. We show representative results with focus on dry temperatures and compare them with analysis data from the European Centre for Medium-Range Weather Forecasts (ECMWF). Although we have available only about 150 CHAMP profiles per day (compared to millions of data entering the ECMWF analyses) the overall agreement between 8 and 30 km altitude is in general very good with systematic differences <0.5 K in most parts of the domain. Pronounced systematic differences (exceeding 2 K) in the tropical tropopause region and above Antarctica in southern winter can almost entirely be attributed to errors in the ECMWF analyses. Errors resulting from uneven sampling in space and time are a potential error source for single-satellite climatologies. The average CHAMP sampling error for seasonal zonal means is <0.2 K, higher values occur in restricted regions and time intervals which can be clearly identified by the sampling error estimation approach we introduced (which is based on ECMWF analysis fields). The total error of this new type of temperature climatologies is estimated to be <0.5 K below 30 km. The recently launched Taiwan/U.S. FORMOSAT-3/COSMIC constellation of 6 RO satellites started to provide thousands of RO profiles per day, but already now the single-satellite CHAMP RO climatologies improve upon modern operational climatologies in the upper troposphere–lower stratosphere and can act as absolute reference climatologies for validation of more bias-sensitive climate datasets and models.

1 Introduction

While there is little doubt that the Earth's surface temperature has risen by about 0.6 K during the twentieth century (IPCC 2001), our knowledge about the temperature evolution in the free atmosphere is still limited (GCOS 2004). Previous estimates of trends in the troposphere and stratosphere have been based on data from radiosondes and from the microwave sounding units (MSU) as well as advanced MSUs (AMSU) on board polar orbiting satellites. Those systems were designed to measure short-term temperature changes in the atmosphere and are not ideally suited for the detection of long-term trends. Radiosonde

U. Foelsche (✉) · M. Borsche · A. K. Steiner · A. Gobiet ·
B. Pirscher · G. Kirchengast
Wegener Center for Climate and Global Change (WegCenter)
and Institute for Geophysics, Astrophysics, and Meteorology
(IGAM), University of Graz, Graz, Austria
e-mail: ulrich.foelsche@uni-graz.at

J. Wickert · T. Schmidt
GeoForschungsZentrum Potsdam (GFZ), Potsdam, Germany

measurements cover almost five decades but they are concentrated above the continental regions of the northern hemisphere and suffer from problems like changes in instrumentation and processing or solar heating of the sensors during daytime (Sherwood et al. 2005). As a consequence no single data product has emerged yet as a generally recognized reference (Seidel et al. 2004).

Microwave sounding units and AMSU data are influenced by instrument and orbit changes, calibration problems, instrument drifts, and insufficient vertical resolution (Anthes et al. 2000). Because of these shortcomings, the magnitude of temperature trends in the troposphere has been under debate for many years (e.g., Christy and Spencer 2003; Vinnikov and Grody 2003; Mears and Wentz 2005).

Radio occultation (RO) data using Global Navigation Satellite System (GNSS) signals have the potential to overcome problems of traditional data sources due to their encouraging combination of high accuracy and vertical resolution, long-term stability due to intrinsic self calibration, global coverage, and all-weather capability. RO data have their highest quality at altitudes between ∼ 8 and ∼ 35 km and are thus well suited for climatologies of the upper troposphere and lower stratosphere (UTLS, which we understand as the altitude range between 5 and 35 km). In the lower troposphere, RO data can be affected by processes like signal multi-path and super-refraction (e.g., Sokolovskiy 2003; Beyerle et al. 2006) and the temperature retrieval requires background information (for more details see Sect. 2.1). The horizontal resolution is low compared to (A)MSU or radiosonde data, but especially for climate applications, where data are averaged anyway, the inherent horizontal averaging of RO data is not a disadvantage.

The RO technique has been developed in the 1960s for the study of planetary atmospheres and ionospheres (see Yunck et al. 2000 for a review). Sensing of the Earth's atmosphere with RO data was first successfully demonstrated with the GPS Meteorology (GPS/MET) experiment. Data from several measurement campaigns (April 1995 to March 1997) proved most of the expected strengths of the technique, like high vertical resolution, high accuracy of retrieved parameters, and insensitivity to clouds (Kursinski et al. 1997; Rocken et al. 1997; Steiner et al. 1999).

The German research satellite CHAllenging Minisatellite Payload for geoscientific research (CHAMP) was launched on July 15, 2000. Continuous RO measurements started in August 2001 (Wickert et al. 2001, 2004). CHAMP RO data thus provide the first opportunity to create RO based climatologies on a multi-year term.

The potential of RO data for climate monitoring has been shown with simulation studies (e.g., Yuan et al. 1993; Steiner et al. 2001; Foelsche et al. 2003; Leroy et al. 2006) and through climatological analyses (Schroeder et al. 2003;

Schmidt et al. 2006; Gobiet et al. 2005b, 2007; Foelsche et al. 2006c; Borsche et al. 2007).

Within the CHAMPCLIM project (Foelsche et al. 2005, 2006c), a cooperation of the Wegener Center in Graz and the GeoForschungsZentrum (GFZ) in Potsdam, we started to build monthly and seasonal mean climatologies of atmospheric microwave refractivity, pressure, geopotential height and temperature, based on CHAMP RO data. Such climatologies, now covering the period from September 2001 until August 2006, are the focus of this paper. The record is still too short to look at trends; therefore we validate the performance with respect to existing climatologies from European Centre for Medium-Range Weather Forecasts (ECMWF), which include data from virtually all traditional sources, like radiosondes and MSU/AMSU satellite instruments.

In Sect. 2 we summarize the properties of RO data, with focus on the CHAMP mission and climate monitoring, and describe the validation data. In Sect. 3 we present example climatologies and error estimates. Sampling errors are a potentially important error source for climatologies derived from single-satellite data. Section 4 deals with this issue, followed by a summary and conclusions in Sect. 5.

2 Data

2.1 Radio occultation data

Radio occultation measurements are performed in an active limb-sounding mode, when radio signals from a GNSS satellite are modified by the Earth's atmosphere and received onboard a satellite in low earth orbit (LEO). From the LEO satellite point of view the GNSS satellite is "occulted" by the atmosphere. The GNSS consists of the U.S. Global Positioning System (GPS) with a nominal constellation of 24 satellites, the Russian GLONASS system and the European Galileo System, which is currently set up and is planned to be operational in 2011 with a nominal constellation of 27 satellites (all present RO missions use signals from GPS satellites only).

A detailed description of the RO technique can be found in the reviews by Kursinski et al. (1997) and Steiner et al. (2001). Foelsche et al. (2006b) provide an overview on the current status of occultation science.

Phase changes (Doppler shift) of the GNSS signals are the basic measurements of the RO technique; these are caused by the respective motions of the transmitting and receiving satellites, by the Earth's ionosphere, and by the neutral atmosphere. The kinematic Doppler effect can be determined and removed via precise knowledge of the satellite's positions and velocities, routinely available from modern precise orbit determination methods (e.g., König

et al. 2002). The effect of the ionosphere is frequency-dependent and can therefore be removed to a high degree using a linear combination of measurements at two GNSS frequencies (ionospheric correction, Vorob'ev and Krasil'nikova 1994). In case of GPS, the two carrier frequencies L1 and L2 are located in the L-band, with wavelengths of 0.19 and 0.24 m, respectively.

The remaining part of the phase change ("atmospheric Doppler") is caused by the refractivity field of the neutral atmosphere. At microwave frequencies, the refractivity N is related to atmospheric pressure p, temperature T, and water vapor partial pressure e, via (Smith and Weintraub 1953):

$$N \equiv 10^6(n-1) = k_1 \frac{p}{T} + k_2 \frac{e}{T^2}, \qquad (1)$$

where n is the index of refraction, k_1 is 77.6 K hPa, and k_2 is 3.73×10^5 K^2 hPa. When atmospheric humidity is small ("dry conditions"), the second term on the right-hand-side of Eq. 1 can be neglected and the microwave refractivity (hereafter referred to just as "refractivity") is directly proportional to the total air density. "Dry conditions" in this sense can be expected everywhere above 8–14 km altitude (details see Sect. 2.4). Atmospheric Doppler profiles and precise orbit data are used to derive bending angle profiles. Via an Abel integral transform (Fjeldbo et al. 1971) under the assumption of local spherical symmetry, these bending angle profiles are converted to refractivity profiles. Under dry conditions, density profiles are then obtained using the first term of Eq. 1, pressure profiles via hydrostatic integration, and temperature profiles using the equation of state for an ideal gas. This process is usually termed "dry air retrieval" (cf. Sect. 2.4). If atmospheric humidity cannot be neglected, auxiliary information is needed to derive specific humidity and temperature (e.g., Kursinski et al. 1997), which is known as "water vapor ambiguity".

Highest quality of RO observations is achieved in the upper troposphere/lower stratosphere region (UTLS). Compared to modern weather analyses CHAMP RO temperature data show an ensemble mean agreement of better than 0.4 K between 10 and 35 km height with a standard deviation of $\sim$1 K at 10 km, increasing to $\sim$2 K at 30 km height (Wickert et al. 2004). Above $\sim$35 km error sources like residual ionospheric effects become important, given the exponential decrease of refractivity with height and therefore a comparatively weak atmospheric signal (e.g., Kursinski et al. 1997). In the lower troposphere the error budget is dominated by horizontal variations of the refractivity and consequent deviations from the spherical symmetry assumption (e.g., Healy 2001a; Foelsche and Kirchengast 2004). In the tropical troposphere below $\sim$5 km altitude, CHAMP RO profiles are affected by a negative refractivity bias, caused by the signal tracking

process currently implemented on GPS receivers and partly by critical refraction (Sokolovskiy 2003; Beyerle et al 2006). Future receivers will have mitigated these weaknesses. Our climatologies are confined to the altitude range, where CHAMP RO profiles with highest quality can be achieved (from 4 to 35 km at high latitudes to 8–35 km in the tropics; see Sect. 3.3), also referred to as the investigated region.

2.2 Utility of RO data for climate monitoring

Atmospheric profiles are not derived from absolute phase measurements but from Doppler shift (phase change) profiles requiring no external calibration and only short-term phase measurement stability over the RO event duration of 1–2 min. The latter is guaranteed by very stable oscillators onboard the transmitter and receiver satellites. GPS signals are controlled by on-board atomic clocks, using Cesium and Rubidium standards. By measuring the phase to a reference GPS satellite during a RO event and observing both the "occulted" and the reference GPS satellite with a ground station ("double differencing") remaining clock errors on the receiving satellite can be removed and the measurement can thus be made traceable to the S.I. (Système International d'Unités) definition of the second, qualifying it as a climate benchmark measurement (Leroy et al. 2006).

With each single RO event intrinsically calibrated this way, and using consistent data processing, long-term stability of derived multi-year climate datasets can be obtained. Data from different sensors and different occultation missions can be combined without need for intercalibration and overlap, as long as the same data processing scheme is used. All RO profiles used in this study have been processed with the same processing scheme.

The long-term stability of RO data could not be tested so far due to the lack of long-time observations. An intersatellite comparison study by Hajj et al. (2004) based on data from CHAMP and SAC-C (Satélite de Aplicaciones Científicas-C), however, showed a remarkable consistency of the data obtained from these two different satellites, with temperature profiles found consistent to within 0.1 K in the mean between 5 and 15 km.

CHAMP and SAC-C are both equipped with very similar receivers ("Black Jack", provided by Jet Propulsion Laboratory), leaving the possibility of small common systematic errors. Future RO missions will help assess whether these results can also be obtained with data from completely different receivers, like the GRAS instrument (GNSS Receiver for Atmospheric Sounding) onboard MetOp (Meteorological Operational satellite, launched in October 2006) (Loiselet et al. 2000).

The RO measurements are characterized by high vertical (~ 0.5 to 1.5 km) and low horizontal resolution (~ 200 to 300 km) (Kursinski et al. 1997). While the former is favorable to accurately resolve structures like the sharp tropical tropopause (Schmidt et al. 2005, 2006) the latter is not a disadvantage for meso- to large-scale climate applications, since profiles would have to be horizontally averaged anyway, so that the "natural averaging" is welcome. The active use of radio signals enables measurements during day and night; the use of L-band signals with wavelengths of ~ 0.2 m ensures that the signals are in general only negligibly influenced by clouds and aerosols.

The geographic distribution of the RO events depends on the geometry of the satellite orbits, primarily on the one of the receiving satellite. Global coverage can only be obtained with a high-inclination orbit of the LEO satellite. This orbit geometry leads, however, to a higher RO event density at high latitudes with comparatively fewer events at low latitudes. Figure 1 shows, as an example for this situation, the typical coverage of RO data from CHAMP (orbit inclination = 87.3°) during one season (top) and the corresponding number of events in zonal bands with 10° latitudinal width (bottom).

Low earth orbit satellites in a low inclination orbit, on the other hand, provide a better sampling at low latitudes, but do not reach global coverage. Figure 1 indicates that even with measurements from a single high-inclination satellite a fairly uniform distribution of RO events during one season can be reached; the average event density over the oceans is as high as over land.

2.3 Radio occultation with CHAMP

CHAMP was launched into an almost circular orbit with an initial altitude of 454 km, which has declined to 350 km until April 2006. Since March 2002, after an initial phase with an increasing number of RO events measured and improvements in the receiver software, it has been recording continuously about 230 RO profiles per day (Wickert et al. 2001; 2004). Out of these ~ 230 daily profiles, about 160 can be successfully processed to phase delays and are of sufficient data quality; ~ 150 of these pass the quality checks during the WegCenter atmospheric profiles retrieval (see Sect. 2.4). All CHAMP RO data are "setting occultations": The signal tracking starts above the atmosphere and the RO event is terminated when the signal is lost, resulting in a decrease in the number of available RO data with decreasing height (e.g., Beyerle et al. 2006). The CHAMP mission is expected to last until 2009; CHAMP RO data thus provide the first opportunity to create continuous RO based climatologies for a multi-year period of >5 years. RO data from other missions like
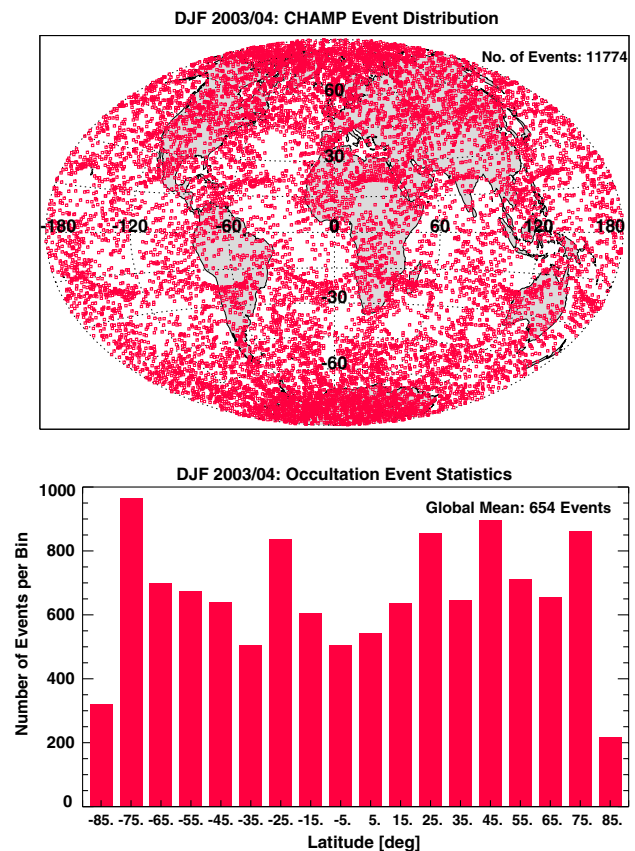

Fig. 1 Geographical distribution of all 11774 CHAMP RO events that passed quality control during the winter season December–January–February (*DJF*) 2003/2004 (*top*). Number of RO events per zonal band (mean number 654) during DJF 2003/2004 (*bottom*)

SAC-C (Hajj et al. 2004) or GRACE (Gravity Recovery and Climate Experiment, e.g., Beyerle et al. 2005; Wickert et al. 2005) are currently only available intermittently in time. In 2006 there is a period of about five weeks (from July 3 to August 8) where no data from CHAMP were available due to technical problems. Fortunately, RO data from the satellite GRACE, which has essentially the same receiver and associated error characteristics as CHAMP (Wickert et al. 2005), were available for this time period. We thus decided to fill the "gap" in the CHAMP record with GRACE data.

2.4 The CHAMPCLIM retrieval

Within the framework of the CHAMPCLIM project (Foelsche et al. 2005) we developed a retrieval scheme at the Wegener Center (Gobiet and Kirchengast 2004; Borsche et al. 2006; Gobiet et al. 2007), which is especially focused on minimizing potential biases of atmospheric parameters and on using background information in a transparent way. The retrieval is based on geometric optics

and ionospheric correction via linear combination of bending angles (Vorob'ev and Krasil'nikova 1994); it starts from RO phase delay data for each occultation event including precise position and velocity information for the GPS and CHAMP satellites, provided by the GFZ Potsdam. The CHAMPCLIM retrieval has been successfully verified in end-to-end simulation studies (e.g., Steiner and Kirchengast 2005) as well as validated against atmospheric analyses from ECMWF and remote-sensing instruments onboard ENVISAT (MIPAS and GOMOS) (e.g., Gobiet et al. 2004, 2005a, 2007).

Background information is integrated into the retrieval process only at one point: At high altitudes, where the errors of RO data are comparatively large, the retrieved bending angle profiles are combined with bending angle profiles derived from co-located ECMWF analysis profiles in a statistically optimal way (Healy 2001b), considering the error characteristics of measurements and background (Gobiet and Kirchengast 2004). The resulting profiles are background-dominated above the stratopause and observation-dominated below 35 km. For the systematic differences between CHAMP and ECMWF (discussed in Sect. 3) the influence of the background is <0.2 K at 30 km and decreases quickly below (Gobiet et al. 2005b).

This approach results in well-defined error characteristics and allows to initialize the hydrostatic integral at very high altitudes (120 km), where the upper-boundary initialization has no effect on the retrieved atmospheric parameters in the height interval under consideration (below 35 km).

In December 2006 ECMWF started to assimilate RO data (Healy 2006). We are thus currently upgrading our processing scheme to no longer use ECWMF analyses but short-range forecasts instead. Using the forecasts will provide sufficiently independent background profiles, as required by the optimal bending angle estimation. Effects of different initialization (analysis vs. forecast) will be crosschecked at least over June 2006–May 2007.

A dry-air retrieval (Syndergaard 1999) is used to derive atmospheric parameters, yielding "dry temperature", which is commonly used in the RO community. Dry temperature, T_{dry}, means that temperature is calculated from the observed refractivity (given by Eq. 1) with the assumption that water vapor is zero, i.e., neglecting the second term of Eq. 1:

$$T_{dry} = k_1 \frac{p}{N} = T \frac{1}{1 + \frac{k_2}{k_1 T} \frac{e}{p}} = T \frac{1}{1 + \frac{k_3}{T} \frac{e}{p}}, \qquad (2)$$

where $k_3 = 4{,}807$ K. Above the lower troposphere (>5 km), assuming a typical upper tropospheric temperature of 240 K and exploiting that $\frac{k_3}{T} \frac{e}{p} << 1$, Eq. 2 can well be approximated by the simple formula:

$$T_{dry} \cong T \left(1 - 20.0 \frac{e}{p} \right) \cong T(1 - 12.4q), \qquad (3)$$

where q (kg/kg) is the specific humidity. For saturated air, the worst case for the approximation, the error of Eq. 3 (compared to the exact Eq. 2) is up to <1 K for $T < 250$ K and well below 0.1 K for $T < 230$ K.

Dry temperatures are colder than physical temperatures as long as e is not exactly 0. At altitudes above 8 km (polar winter) and 14 km (tropics) this difference is always well below 0.1 K and T_{dry} is equivalent to T. In the lower troposphere, however, it can reach several tens of kelvins.

In the current version of the CHAMPCLIM retrieval (v2.3) all altitudes are computed above the geoid, i.e., are mean-sea-level (MSL) altitudes. All retrieved profiles are assigned with a quality flag (QF), only high-quality profiles with QF 0 are used for climatologies. Tropopause parameters including the lapse rate tropopause altitude and temperature and the cold point tropopause altitude and temperature are calculated for each profile.

2.5 ECMWF analysis data

The integrated forecasting system (IFS) of the ECMWF operationally produces daily analyses for four time layers, 00, 06, 12, and 18 UT (universal time), by dynamically combining a short-range forecast with observational data via four-dimensional variational assimilation (ECMWF 2004). Since October 2003 Advanced Infrared Sounder (AIRS) radiances are included in the analyses (ECMWF 2003). On February 1, 2006 a major resolution upgrade has been implemented at ECMWF with a vertical resolution increase from 60 to 91 levels and a raise of the model top from 0.1 to 0.01 hPa. The horizontal resolution has increased from T511 (spectral representation with triangular truncation at wave number 511) to T799 (ECMWF 2005), allowing more atmospheric activity to be represented. We decided to use ECMWF analysis fields as reference since they have widely recognized quality, adequate spatial and temporal resolution and contain a vast amount of observations, assimilated in a statistically optimal way.

The comparison between CHAMP and ECMWF is based on difference profiles. For each CHAMP RO profile we extracted a co-located vertical ECMWF profile from the nearest time layer of the analysis at the mean location of the (non-vertical) RO profile, using spatial interpolation. We define the mean location as the latitude and longitude of the point, where the straight-line connection between transmitting and receiving satellite during the occultation event touches the Earth's ellipsoidal surface (corresponding to the

tangent point location of real RO profiles at about 12–15 km altitude).

3 Seasonal climatologies

3.1 Setup of climatologies

CHAMP climatologies are obtained by "binning and averaging". All CHAMP profiles in a prescribed geographic domain ("bin") are sampled and averaged (weighted by the cosine of the latitude), using a common altitude grid. The mean dry temperature profile in each bin is given by

$$\overline{T_{\text{dry}}(z)} = \frac{1}{\sum_{i=1}^{N_{\text{prof}}(z)} \cos(\varphi_i)} \sum_{i=1}^{N_{\text{prof}}(z)} T_{dry_i}(z, \varphi_i) \cos(\varphi_i), \qquad (4)$$

where N_{prof} is the number of profiles in each bin, which decreases with decreasing height in the troposphere (see Sect. 2.3). We use "fundamental" zonal bins with 5° latitudinal width to build zonal mean monthly climatologies. Our basic latitudinal resolution (used for the results shown here) is 10°, each of the 18 latitude bands (pole to pole) contains two fundamental bins, and the mean profiles for these two bins are averaged, weighted with the surface area of the respective bin. This approach slightly reduces the effect of uneven sampling within the latitude bands. Seasonal climatologies are obtained by averaging over three months. Two hundred meter vertical spacing was chosen for the altitude gridding.

At this latitudinal resolution the effect of cosine-weighting (Eq. 4), which accounts for area changes between meridians at varying latitudes, is minimal, but it starts to be relevant for larger-area averages. Including also longitudinal resolution is feasible, but the quality of the climatologies depends on the spatial distribution of the RO events, which can be unfavorable in certain time intervals. For single-satellite monthly and seasonal climatologies we recommend to use zonal mean fields.

The quasi-operational data stream of CHAMP RO data started in March 2002; from September 2001 until February 2002 the amount of available RO profiles was considerably smaller (about 100 profiles per day), but still sufficient to build climatologies on a seasonal zonal mean basis. Altogether the climatologies thus cover a period of over 5 years from September 2001 to February 2007.

In the future we will operationally include also data from the non-continuous SAC-C and GRACE RO missions, as well as data from the operational MetOp mission and the FORMOSAT-3/COSMIC system (Constellation Observing System for Meteorology, Ionosphere, and Climate), a Taiwan/U.S. RO mission consisting of six receiving satellites, which was successfully launched in April 2006 (Rocken et al. 2000; Wu et al. 2005). COSMIC is expected to obtain ∼2,500 setting and rising occultations per day, providing a very valuable database for RO based climatologies. But already with continuous RO data from a single satellite, like CHAMP, high-quality climatologies can be obtained as discussed below. We have, however, to take into account and to carefully understand the error due to spatial and temporal undersampling of the true evolution of atmospheric fields, which has been identified as a potential major error source for single-satellite RO climatologies with the aid of simulation studies (Foelsche et al. 2003).

3.2 Estimation of the sampling error

Even with perfect observations at the occultation locations the "measured" climatologies would differ from the "true" ones as the sampling through occultation events is discrete and not dense enough to capture the entire spatio-temporal variability of the atmosphere. Under the assumption that the ECMWF analysis fields and the spatio-temporal variability per time layer (4 time layers per day) approximately represent the "true" state of the atmosphere, we can estimate the sampling error by comparing climatologies derived from the ECMWF profiles at the RO locations with climatologies derived from the 4D ECMWF fields using the complete field. The dry temperature sampling error profile in each bin is estimated as:

$$\Delta T_{\text{dry}}^{\text{sampling}}(z) = \frac{1}{N_{\text{prof}}} \sum_{i=1}^{N_{\text{prof}}} T_{\text{dry}_i}^{\text{true}}(z) - \frac{1}{N_{\text{grid}}} \sum_{j=1}^{N_t} \sum_{k=1}^{N_\varphi} \sum_{l=1}^{N_\lambda} T_{\text{dry}_{jkl}}^{\text{true}}(z),$$
$$(5)$$

where N_{prof} is the number of profiles in the bin, the summation on the right hand side is over all N_λ longitude and N_φ latitude grid points in the bin and over all N_t time layers within the selected time interval (month or season), $N_{\text{grid}} = N_\lambda N_\varphi N_t$. Cosine weighting (Eq. 4) and decrease of ensemble members with decreasing height (Sect. 2.3) are taken into account but are not explicitly written in Eq. 5 for the sake of simplicity.

3.3 Dry temperature results for an example season

Figure 2 displays different CHAMP climatology products for a typical season, the northern winter season December–January–February (DJF) 2003/2004, resulting from the RO event distribution shown in Fig. 1. The seasonal CHAMP dry temperature climatology is shown in Fig. 2a, the corresponding ECMWF climatology, based on the full 3-D

grid, in Fig. 2b. The vertical range of all fields shown extends from 0 to 35 km altitude. Additionally, the climatologies are cut off at the lower end at varying height increasing from the poles towards the equator.

From the poles to 60° latitude they reach down to 4 km, the cut-off height then increases over the mid latitude bins to 8 km at low latitudes (equator to 30° north and south). Within 60°–30° the cut-off heights are 5 km (60°–50°), 6 km (50°–40°), and 7.5 km (40°–30°). The reason for the cut-off strategy is the biased sampling in the lower troposphere caused by different penetration depths of the individual profiles (see Sect. 4.4 for a detailed discussion).

The systematic difference (Fig. 2c) is based on difference error statistics for each of the 18 bins, using a collocated ECMWF profile (Sect. 2.4) for each CHAMP RO profile (taking CHAMP as reference). The ensemble averages of the CHAMP and ECMWF profiles in each bin are computed via Eq. 4. Note that CHAMP bending angles have been combined with ECMWF-derived bending angles in the upper stratosphere (Sect. 2.4). At 35 km altitude,

however, the background influence has diminished enough to allow for considerable differences between CHAMP and ECMWF.

Above 30 km ECMWF is systematically colder than CHAMP almost everywhere; this feature is typical for all seasons considered so far, with maximum deviations of −1.5 K to about −2 K. Any remaining background influence would imply that the "true" differences are even larger. In this altitude range ECMWF analyses are only weakly constrained by observations but individual CHAMP profiles show larger errors as well and a systematic component of CHAMP errors cannot be completely ruled out. First results based on climatologies using RO data from SAC-C as well as FORMOSAT-3/COSMIC (U. Foelsche et al., Assessing the Climate Monitoring Utility of Radio Occultation Data: From CHAMP to FORMOSAT-3/COS-MIC, *Terrestrial Atmospheric and Oceanic Physics*, revised manuscript, 2007, hereinafter referred to as Foelsche et al., revised manuscript, 2007) show a close agreement with CHAMP data, including the 30–35 km altitude range, but at
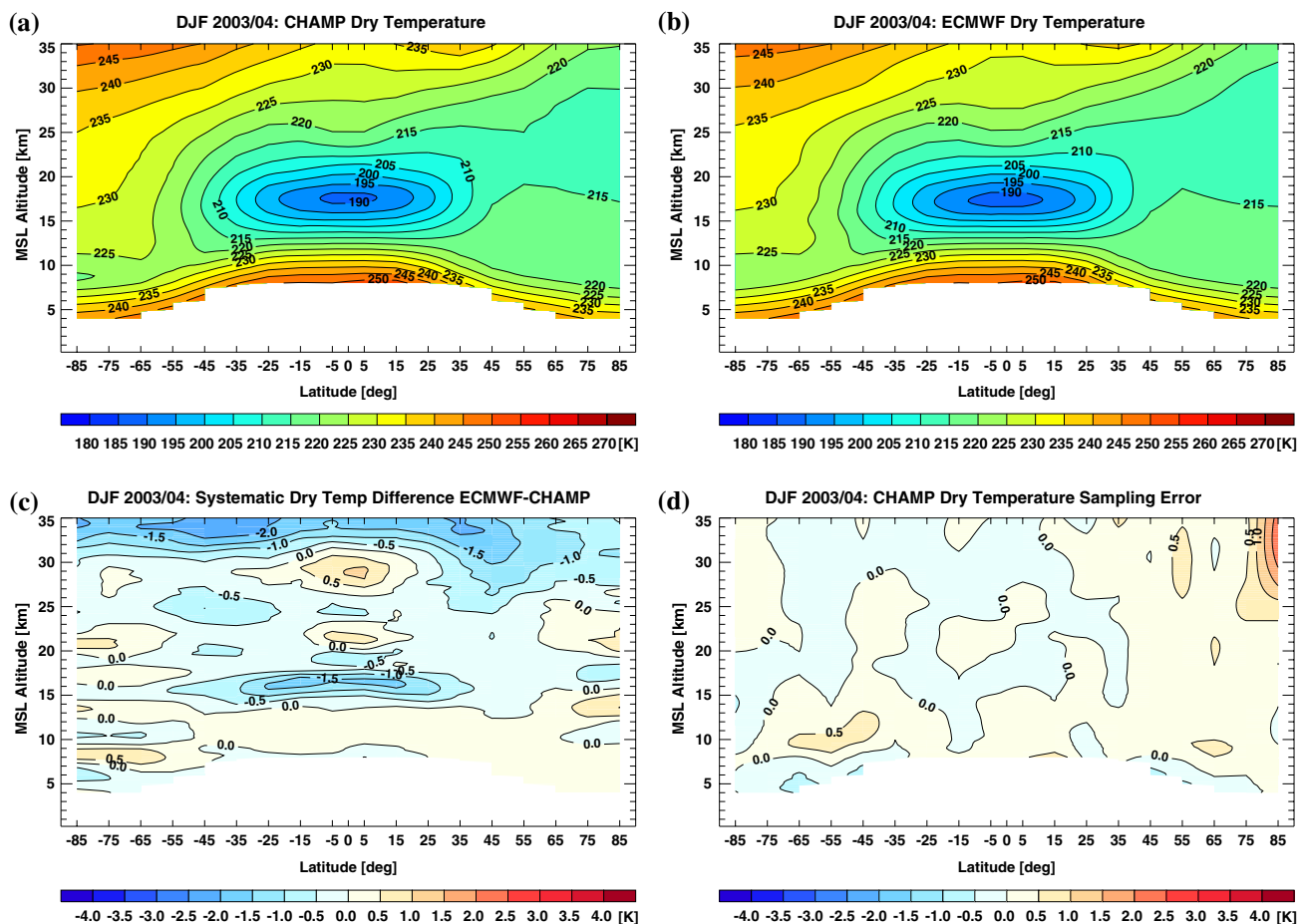

Fig. 2 Zonal mean dry temperature fields for the example season DJF 2003/2004: CHAMP dry temperature (**a**), ECMWF dry temperature (**b**), systematic difference, taking CHAMP as reference (**c**), and estimated CHAMP sampling error (**d**)

the current stage we assume that the systematic difference is most probably due to errors in both CHAMP and ECMWF.

In the height range, where RO data have the highest quality (~ 8 to ~ 30 km), the agreement between CHAMP and ECMWF is, in general, very good: The absolute systematic difference is <0.5 K, occasionally peaking at 1 K. However, one feature is prominent throughout the seasons:

The tropical tropopause region in the CHAMP-derived fields is consistently warmer than in the ECMWF analyses, the differences exceed 1.5 K. The reason is not simply a better height resolution of CHAMP compared to ECMWF, in this case we would expect the opposite sign for the difference with CHAMP observing colder tropopause temperatures. The systematic difference is caused by a weak representation of atmospheric wave activity and tropopause height variability in ECMWF fields. It is typical for all seasons from SON 2001 until DJF 2005/2006, occasionally exceeding 2 K. A detailed discussion can be found in Borsche et al (2007).

A smaller, but also consistent feature appearing in all seasonal climatologies, is a positive deviation at low latitudes between ~ 27 and ~ 31 km altitude, reaching typical values of +0.5 K to +1 K and being part of a wave-like deviation pattern in the tropical lower stratosphere. This feature has not been analyzed so far and deserves further consideration; currently we speculate it is, similar to the Antarctic winter deviation pattern discussed in Sect. 3.4 below, due to residual biases in the ECMWF analyses.

The estimated (absolute) sampling error in DJF 2003/2004 (Fig. 2d) is only occasionally larger than 0.5 K. This situation is representative for latitudes between 60°S and 60°N for all seasons, sampling errors in polar bins can be larger, predominantly in spring and fall (see Sect. 4.2). These occasional sampling error increases can be explained by clustering of RO events and uneven sampling of the polar vortices. The mean (absolute) value for the sampling error in the UTLS is <0.3 K for monthly means and <0.2 K for seasonal zonal means (Pirscher et al. 2007).

Dry temperature climatologies and corresponding error fields for all seasons from December 2001 until February 2005 as well as monthly climatologies for the year 2003 are presented in Foelsche et al. (2006a). First results on RO climatologies from FORMOSAT-3/COSMIC (U. Foelsche et al., revised manuscript, 2007) indicate excellent agreement between RO climatologies from different COSMIC satellites as well as between data from CHAMP and COSMIC. After subtraction of the estimated respective sampling error, seasonal temperature climatologies derived from different COSMIC satellites agree to within <0.1 K almost everywhere between 8 and 35 km altitude.

3.4 Temporal evolution (summer seasons)

CHAMP dry temperature zonal and seasonal mean fields for the summer seasons June–July–August (JJA) 2002–2006 are displayed in Fig. 3 (left panels). The most prominent features are the cold tropical tropopause region and the cold austral polar vortex during southern winter, where temperatures down to below 182 K can be found during JJA 2003. While the large-scale features are remarkably constant over this 5-year period, interannual variations can clearly be seen. In the tropical stratosphere there is a clear temperature variation with a 2-year period (most easily visible when looking at the 230 K isotherm), which is obviously linked to the Quasi Biennial Oscillation (QBO) (e.g., Ramaswamy et al. 1999). Also the temperatures in the Antarctic polar vortex show variations with a 2-year period, a relation to the QBO seems plausible. During JJA 2002, for example, the Antarctic polar vortex was much warmer than during JJA 2003, with temperatures above 185 K everywhere.

The systematic differences to ECMWF (taking CHAMP as reference) are shown in the right panels of Fig. 3. Apart from the expected differences above 30 km and in the tropical tropopause region (Sect. 3.3) there is a remarkable pattern: A wave-like bias structure with a magnitude of several degrees in the southern winter polar vortex region. It has been discovered based on results from the CHAMPCLIM testbed season JJA 2003 (Fig. 3c, d) as described by Gobiet et al. (2005b).

This feature is far beyond the error characteristics of RO data and can be clearly attributed to the ECMWF data. It is caused by deficiencies in the representation of the austral polar vortex in the analysis fields. A plausible explanation is that ECMWF model errors at high altitudes are partly resolved by satellite radiance data. The assimilation of these data with coarse height resolution, however, causes the wave-like response of the analysis scheme, where the amplitude decreases with height (A. Simmons, ECMWF, personal communication, 2004).

The largest differences in JJA 2003 amount to −2.5 and +3.5 K, respectively. In JJA 2002, a year with a warmer polar vortex (Fig. 3a) the situation is qualitatively similar, but the largest deviations do not exceed −2 and +2.5 K, respectively.

During JJA 2004 this bias structure (Fig. 3f) is again less pronounced than in JJA 2003 (max. differences of −2 and +2 K, respectively). We attributed this effect to the addition of new data (AIRS radiances) to the ECMWF analyses in October 2003 (ECMWF 2003) and changes in the assimilation scheme like bias adjustments of satellite data (A. Simmons, ECMWF, personal communication, 2005).

Given these improvements it is surprising to see the results for JJA 2005 (Fig. 3g, h): The bias structure is
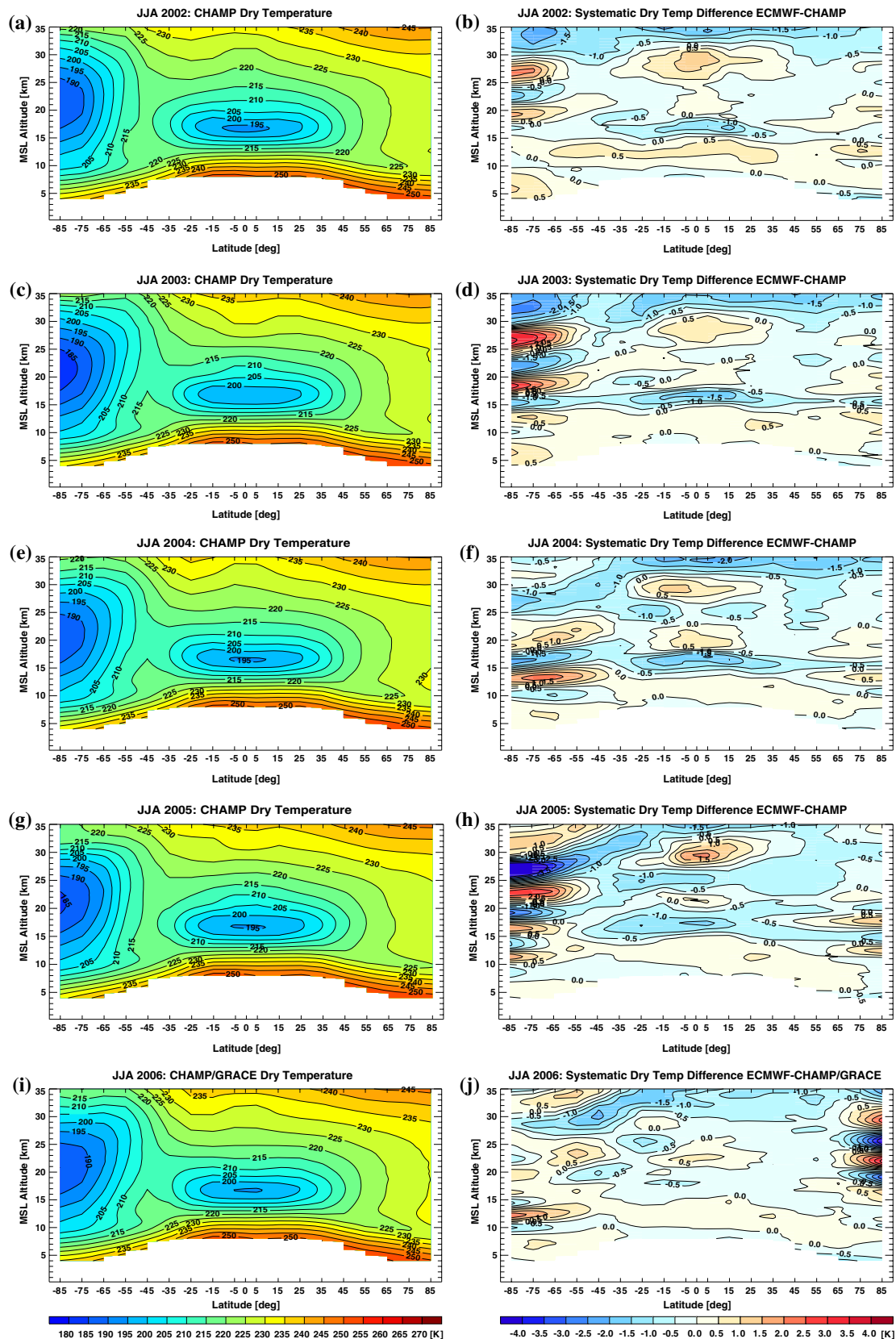
Fig. 3 CHAMP seasonal and zonal mean dry temperature fields for the summer seasons June–July–August (*JJA*) 2002–2006 (*left panels*) and corresponding systematic differences to ECMWF, taking CHAMP as reference (*right panels*)

stronger than in all observed summers before, with deviations exceeding −4 and +3 K, respectively. Interestingly, the phase has changed the sign. In monthly mean zonal mean fields (not shown), similar but less pronounced features can be found in May and, to a smaller extent, in September, which also influence the seasonal climatologies for spring and fall.

During JJA 2006 the climate record is composed of data from CHAMP and GRACE (see Sect. 2.3). The systematic difference for June + August between ECMWF and CHAMP alone (not shown) displays essentially the same large scale features as Fig. 3j, only at small scales there is more variability. Compared to all previous seasons shown, the ECMWF data of JJA 2006 are entirely based on the new model system (see Sect. 2.5) with higher vertical resolution (91 vertical levels) and thus less truncation of atmospheric wave activity (ECMWF 2005).

The systematic difference between ECMWF and CHAMP+GRACE (Fig. 3j) shows two striking features: The large systematic difference in the tropical tropopause region, which was typical for all previous seasons, has almost entirely disappeared. The Antarctic winter bias structure has also almost disappeared, but there is now a similar bias structure over the Arctic, reaching values of −4 and +3.5 K, respectively.

Assimilation experiments (Healy and Thépaut 2006) suggested that assimilating CHAMP RO data into ECMWF analyses would improve these problems and the operational assimilation of FORMOSAT-3/COSMIC RO data at ECMWF (Healy 2006) in fact reduces the oscillations considerably.

These results strongly support our conclusion that the systematic differences between ECMWF and CHAMP data below 30 km are mainly caused by the ECMWF analyses and not by CHAMP (Sect. 3.3), underpinning the value of RO data to act as absolute reference climatologies for other more bias-sensitive datasets.

3.5 Estimation of the climatological error

The observational error of the CHAMP climatologies is given by the root mean square error (r.m.s.) of the mean. For each altitude level in each bin the observational dry temperature error, ΔT_{dry}^{obs}, is a combination of the systematic error of the mean, ΔT_{dry}^{bias}, and the standard deviation of the mean:

$$\Delta T_{dry}^{obs} = \left[\left(\Delta T_{dry}^{bias} \right)^2 + \left(\frac{\Delta T_{dry}^{stddev}}{\sqrt{N_{prof}}} \right)^2 \right]^{1/2}, \qquad (6)$$

where ΔT_{dry}^{stddev} is the standard deviation of the N_{prof} individual CHAMP observations.

CHAMP standard deviations show a quite uniform behavior and can be represented by simple analytical models (Steiner et al. 2006). Error statistics of atmospheric difference profiles (with ECMWF profiles as reference) show dry temperature standard deviations which increase from 1 K at ∼14 km altitude to ∼2.5 K at 4 and 35 km altitude, respectively. Taking the uncertainties of ECMWF into account, these numbers are reduced and the estimated CHAMP-only values range from 0.8 to 2 K (Foelsche et al. 2006a). For seasonal zonal mean climatologies N_{prof} is only occasionally <400, leading to an error reduction by a factor of at least 20 almost everywhere. In our example season DJF 2003/2004 (see Fig. 1), N_{prof} is 654 on average, values <400 occur only in the small polar cap bins. The standard deviation of the mean can thus be expected to be <0.1 K almost everywhere, even at 35 km altitude.

The observational error (r.m.s. of the mean) is therefore clearly dominated by the systematic error of the mean (bias). We note that the systematic differences between CHAMP and ECMWF (Figs. 2, 3, 4) contain a considerable contribution of the ECMWF analyses themselves, as discussed for prominent features in Sects. 3.3 and 3.4, where most differences exceeding 0.5 K can be attributed to ECMWF. We therefore suppose that a value of 0.5 K is a reasonable and conservative upper-limit estimate for the observational error of CHAMP climatologies within ∼8 to ∼30 km altitude. We recall for context the results by Hajj et al. (2004) showing that ensembles of RO profiles from CHAMP and SAC-C agree to within 0.1 K in the mean between 5 and 15 km (see Sect. 2.2). RO data from the recently launched FORMOSAT-3/COSMIC mission and from the GRAS instrument onboard MetOp will allow to determine the systematic error of RO climatologies with higher precision, based on extensive inter-validation.

The total climatological error, ΔT_{dry}^{clim}, is a combination of the observational error (Eq. 6) and the sampling error (Eq. 5). As these two error sources can be assumed uncorrelated we obtain:

$$\Delta T_{dry}^{clim} = \left[\left(\Delta T_{dry}^{obs} \right)^2 + \left(\Delta T_{dry}^{sampling} \right)^2 \right]^{1/2}. \qquad (7)$$

If the observational error is indeed closer to the estimate suggested by the results by Hajj et al. (2004) we can assume that the total error of single-satellite RO climatologies is dominated by the sampling error. Taking an average CHAMP sampling error of 0.2 K in the UTLS for seasonal zonal means (Sect. 3.3) and average bias estimates of 0.5 K (conservative), 0.3 K (medium), 0.1 K (potential by measurement principle), Eq. 7 gives a total climatological error of ∼0.5 K (∼0.4, ∼0.2 K), respectively, for those three estimates. Future work will further refine quantification of these errors but overall it seems valid to

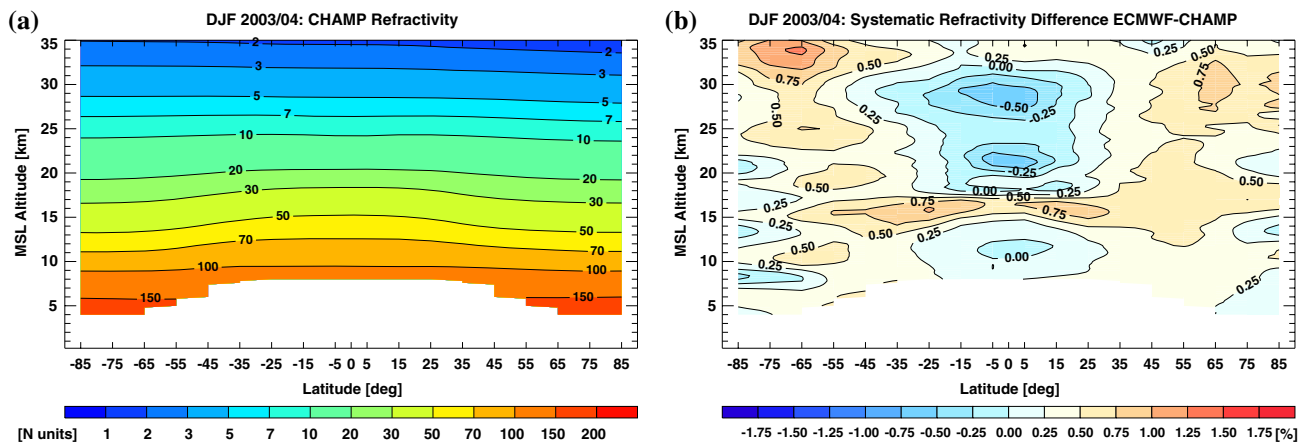**Fig. 4** Seasonal mean, zonal mean CHAMP refractivity for DJF 2003/2004 (**a**) and relative systematic difference ECMWF–CHAMP with CHAMP as reference (**b**)

think of the accuracy of this new type of UTLS temperature climatologies as being better than 0.5 K in the investigated region below 30 km.

3.6 Example climatologies of refractivity and geopotential height

In addition to CHAMP dry temperature fields we prepare climatologies of refractivity, pressure, and geopotential height. The seasonal zonal mean refractivity field for the example season DJF 2003/2004, resulting from the event distribution shown in Fig. 1, is displayed in Fig. 4a. In the investigated region the refractivity depends primarily on the dry air density (Eq. 1), the general feature is thus an exponential decrease of refractivity with altitude. Refractivity is a dimensionless quantity; it is common practice to use the term "N units". Large-scale features and interannual variability are less obvious than in case of dry temperature. (Microwave) refractivity is up to now not a very common atmospheric parameter outside the RO community, but refractivity climatologies are a valuable complement to common climate records such as of temperature since refractivity responds differently in a changing climate and has been identified as a good indicator for climate change (Vedel and Stendel 2003). Furthermore, it is a quantity, which is calculated at an earlier step than temperature in the RO retrieval chain (i.e., is closer to the observations) and its retrieval does not require additional information in the (lower) troposphere (see Sect. 2.1).

Given the exponential decrease of refractivity with altitude we prefer to show the relative systematic difference compared to ECMWF in (%), again with CHAMP as reference (Fig. 4b). It mirrors the corresponding (absolute) dry temperature difference (Fig. 2c), with negative deviations where the temperature deviations are positive and

vice versa (see Eq. 1), which roots in the fact that fractional air density changes are (negatively) proportional to absolute temperature changes, as shown in detail by Rieder and Kirchengast (2001). ECMWF refractivities in the tropical tropopause region, as example, are higher than corresponding CHAMP refractivities. The refractivity sampling error is not explicitly shown since it does not differ qualitatively from the dry temperature sampling error.

Also the geopotential height of pressure surfaces has been identified as a good indicator for climate change (Leroy 1997). The seasonal and zonal mean geopotential height field for DJF 2003/2004 is shown in Fig. 5a, the corresponding systematic difference ECMWF-CHAMP in Fig. 5b. The fields are displayed as a function of "pressure altitude" z_p in units "pressure km" [km]. z_p is defined as $z_p(\text{km}) = -7(\text{km}) \cdot \ln(p(\text{hPa})/1013.25)$. It is closely aligned with geometrical altitude z since 7 km is a good average atmospheric scale height below the mesopause (>0.01 hPa) and 1013.25 hPa is the (global mean) standard surface pressure. It is thus a convenient substitute for a log–pressure coordinate.

Systematic geopotential height (and pressure) differences show generally a smoother behavior than dry temperature or refractivity due to the hydrostatic integration. The results for the example season (Fig. 5b) display a "tripole" feature, which is also characteristic for all other seasons analyzed so far. ECMWF geopotential heights are systematically higher than CHAMP at mid- to high latitudes in both hemispheres, but lower at low latitudes above the tropopause. After the changes at ECMWF in Feb 2006 (Sect. 2.5) the overall structure is still qualitatively the same. The reason for this stationary systematic difference is under investigation. Our current understanding is that the major source is a difference in the representation of the Earth's reference surface (Ellipsoid), which will be mitigated in future processing versions.
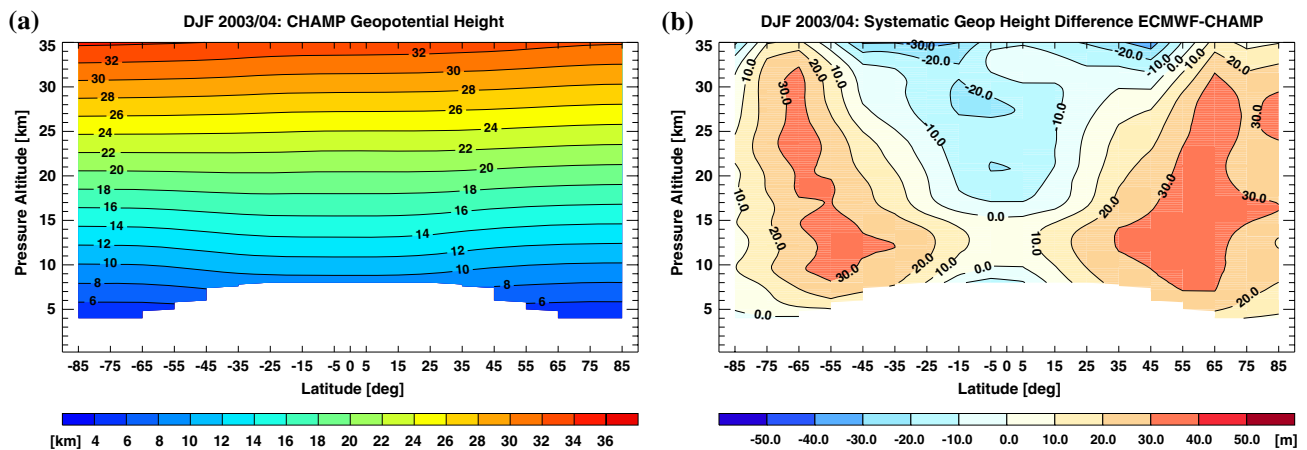
(a)

(b)

Fig. 5 Seasonal mean, zonal mean CHAMP geopotential height for DJF 2003/2004 (**a**) and relative systematic difference ECMWF–CHAMP with CHAMP as reference (**b**)

Regarding pressure fields, the relative pressure errors (not shown) closely mirror absolute geopotential height errors, due to the physical definition of geopotential height of pressure levels (e.g., Leroy 1997).

We have shown that in a changing climate different atmospheric parameters are sensitive in different regions of the atmosphere (Foelsche et al. 2006c). Climate monitoring with RO data should therefore, in principle, comprise all parameters that can be retrieved with the RO technique.

3.7 Tropopause parameters

Tropopause parameters (like altitude and temperature) are as well promising indicators of climate change (e.g., Schmidt et al. 2005). We started to analyze the CHAMP tropopause record, the results being reported by Borsche et al. (2007). Key findings of that study are: NCEP (National Centers for Environmental Prediction) reanalysis lapse rate tropopause (LRTP) temperatures exhibit warm deviations of about 4 K against CHAMP until the end of 2004, decreasing to about 2 K from 2005 onwards; EC-MWF LRTP temperatures were systematically colder than CHAMP by ∼2 K but converged to CHAMP values after February 2006, when a major improvement of the ECMWF model system became effective (see Sect. 2.5 and 3.4). Initial results on tropopause temperatures and altitudes derived in a multi-satellite approach from CHAMP, GRACE, SAC-C, and FORMOSAT-3/COSMIC (U. Foelsche et al., revised manuscript, 2007) show remarkable inter-satellite consistency of tropopause temperatures and altitudes (<0.2−0.5 K, <50–100 m) and indicate that data from different RO missions can indeed be combined without need for inter-calibration.

Tropopause parameters are routinely computed during the profile retrieval process. Work on maps of tropopause

altitude and temperature is currently on going; these products will complement the atmospheric fields.

4 Sampling error

In satellite climate observing systems, characterization and understanding of sampling errors always deserves particular care to clearly evaluate the climate monitoring quality. In this section we focus on the errors introduced in single satellite RO climatologies by uneven sampling in space (Sect. 4.1), time (Sect. 4.2), and local time (Sect. 4.3), and on the specific effect of "dry sampling" (Sect. 4.4). The sampling errors are estimated based on ECMWF fields as described in Sect. 3.2.

4.1 Spatial distribution of RO events

The geographical distribution of CHAMP RO events is determined by the geometry of the orbits of CHAMP and of the transmitting GPS satellites. The left panels of Fig. 6 show a typical situation for monthly zonal mean fields (June 2003) with comparatively well-distributed RO events (a) and corresponding small sampling errors (e), which are < 0.5 K almost everywhere (estimated by the approach introduced in Sect. 3.2).

The CHAMP RO event density (c) at high latitudes is higher than at low latitudes (see Sect. 2.2), with exception of the small polar caps. Comparatively smaller temperature variations in the low latitude bins, however, prevent the sampling error from increasing.

In April 2003 (right panels of Fig. 6), the geometry of the satellite orbits leads to a remarkable clustering of RO events (b). The number of RO events in April (3925) is not much smaller than in June (4430), but the number of
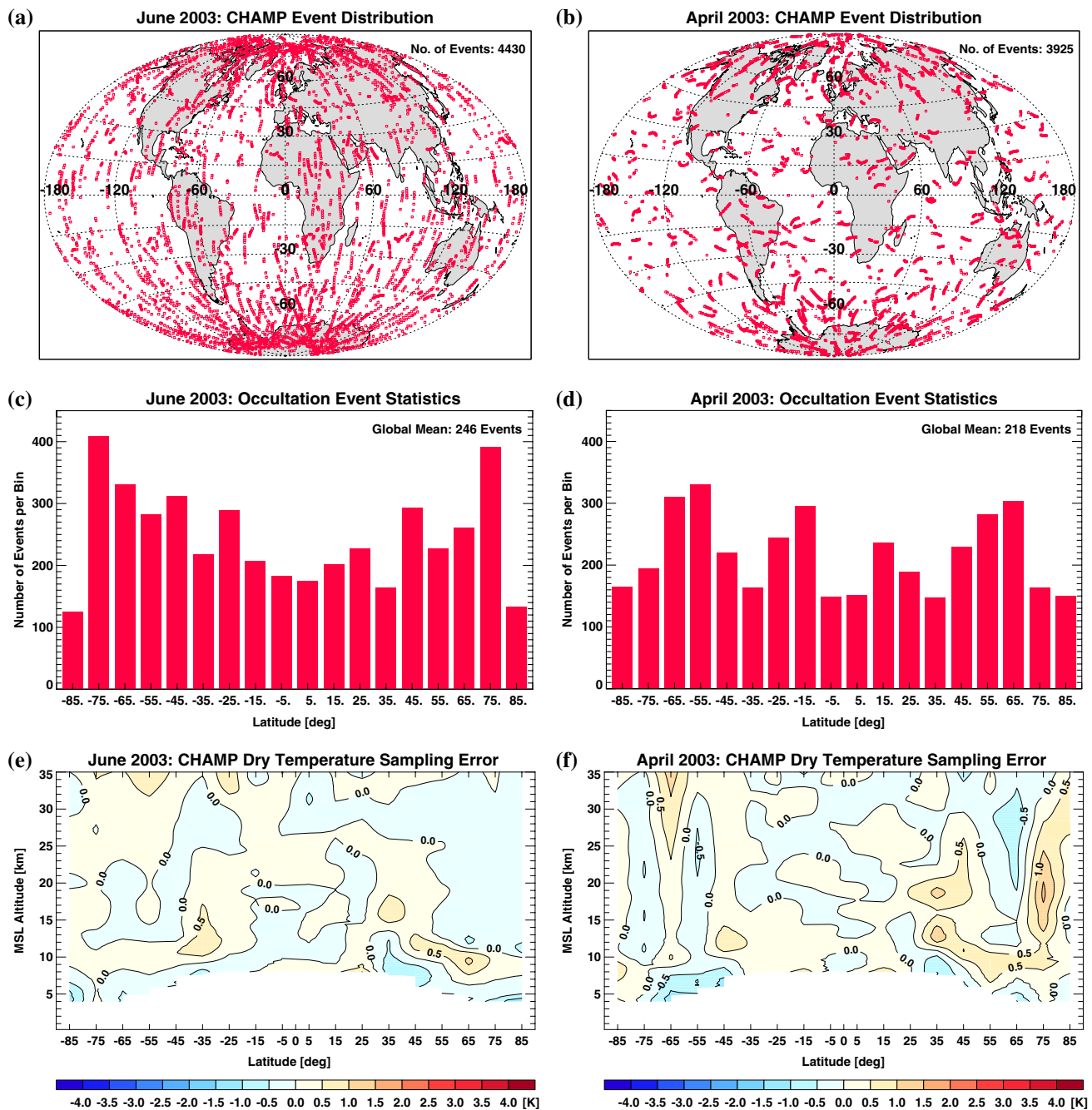
(a)

(b)

(c)

(d)

(e)

(f)

Fig. 6 Distribution of CHAMP RO events (*top*), number of events per bin (*middle*), and corresponding estimated dry temperature sampling error (*bottom*): June 2003 (*left*), April 2003 (*right*)

independent bits of information is considerably reduced. The corresponding sampling error is thus markedly larger (f). A similar (less pronounced) situation is encountered in April 2002 and 2004 (not shown). This problem due to certain cycles in orbit geometry cannot be easily overcome, since the distribution of RO events cannot be affected, but our strategy of co-monitoring of the sampling error provides a valuable means to identify and flag time intervals and geographic regions that are subject to larger sampling errors than the nominal ones. More occultations per day as upcoming in the future from multiple RO satellites will essentially mitigate these effects.

4.2 Temporal evolution

Figure 7 shows the temporal evolution of the monthly dry temperature sampling error from September 2001 until

November 2006 in a latitude bin which is particularly affected by uneven sampling (70°N–80°N). We can see that large sampling errors occur only intermittently in time, dominantly in winter, when the polar vortex is not adequately represented. The large negative deviations in December 2001 and February 2002 fall in the period when the CHAMP RO data stream was still limited before its full start by March 2002. Within February 2002, for example, the number of occultation events decreases considerably, leading to a large error through uneven temporal sampling. After February 2002 the sampling errors are generally much smaller, those in March and April 2003, e.g., almost cancel when building the MAM 2003 seasonal climatology. Individual months that are suspect to higher sampling errors, like February 2005, can be clearly identified with our estimation method. Near the polar tropopause generally a slightly increased sampling error is visible at altitudes of about 8–11 km, indicating that multiple RO satellites will be particularly welcome also here.

4.3 Local time component

Concerning temperature data retrievals, the local time of the occultation events plays an essential role because of distinct daily temperature variations. A (slow) shift of the local time of occultation events could produce a temperature trend without physical relevance—simply caused by an inappropriate sampling interval (see, e.g., Kirk-Davidoff et al. 2004).

The orbit geometry of the CHAMP satellite leads to a continuous change in its equator crossing time with a rate of ∼1 h per 11 days, which is called a drifting orbit. The RO events are clustered around the local times of the ascending and descending nodes of the satellite orbit. In May 2003, for example, there are peaks of RO local times in the early morning (between ∼3 and ∼6 am) and afternoon (∼3 to ∼6 pm), respectively. One month later,

the peaks have moved ∼3 h "back" to near midnight (∼12 pm to ∼3 am) and near midday (∼12 am to ∼3 pm), respectively.

The effect of uneven local time sampling decreases when seasonal or annual means are considered, but even seasonal means (90–92 day period) do not yet fully sample the diurnal cycle (the diurnal cycle is completely sampled within ∼130 days). The local time component of the CHAMP dry temperature sampling error is, however, small compared to the one caused by the uneven geographical distribution. It can be estimated to be on average 0.1 K for monthly zonal means, ∼0.06 K for seasonal zonal means and ∼0.03 K for annual seasonal means (see Pirscher et al. 2007 for a detailed discussion).

RO data from satellites in sun-synchronous orbits (like SAC-C and MetOp) are not subject to systematic changes in the local times of the observations. If there is a (small) systematic component of the local time sampling error, it will remain constant in time (Pirscher et al. 2007).

4.4 Dry sampling error

In Fig. 8 we show the estimated dry temperature sampling error for the summer season JJA 2003 for the entire height domain without the tropospheric cut-off nominally applied (Sect. 3.3). It is <0.5 K almost everywhere above 8 km. In the lower troposphere at low and mid-latitudes however, there is a large "warm" sampling error for dry temperatures, reaching values of over +15 K in the tropics. This RO specific feature can be understood as a selective "dry sampling error" since the RO receiver tracking of CHAMP signals and the geometric optics retrieval tends to stop at higher altitudes in moist compared to dry atmospheric conditions. The lowest part of the RO ensembles is therefore biased towards dry conditions (with smaller refractivities), resulting in a systematic under-representation of the "true" mean refractivity (see Eq. 1, Sect. 2.2).

Fig. 7 Temporal evolution of the monthly CHAMP dry temperature sampling error at high northern latitudes (70–80°N)
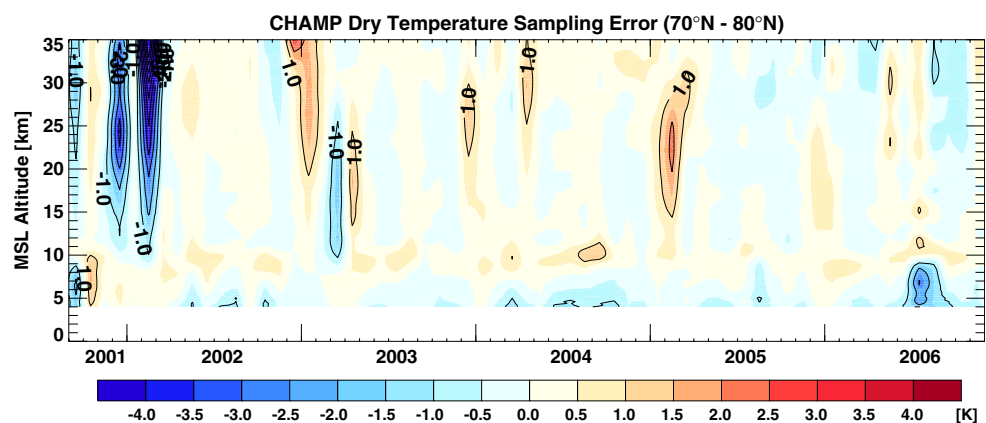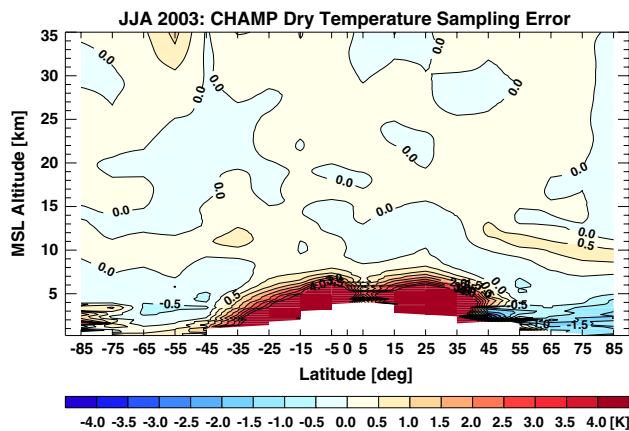
Fig. 8 Estimated dry temperature sampling error for the summer season JJA 2003. The cut-off region (*white*) corresponds to height intervals where the remaining ensemble of RO events has decreased to <10 in the respective bin

When the refractivities are converted to dry temperatures, this systematic error maps into significantly warm-biased mean dry temperatures (see Eq. 2, Sect. 2.3).

This effect is most pronounced at low latitudes, where the event density is particularly low (see Figs. 1, 6a,b). The implementation of a wave optics algorithm (Gorbunov 2002; Jensen et al. 2003) in the WegCenter retrieval will reduce this "dry sampling error", but it will remain an important error source for RO based climatologies at low latitudes below ∼8 km. This "dry sampling error" is the main reason for the cut-off criterion used for operational CHAMP dry-retrieval climatologies, described in Sect. 3.3. At the same time the cut-off reflects the increasing relevance of moisture perturbation to dry temperature profiles with decreasing height, most prominent at low latitudes. Also for this reason cutting of T_{dry} profiles is sensible, since below the cut-off height T_{dry} begins to strongly deviate from the physical temperature T (Eq. 3, Sect. 2.4).

5 Summary, conclusions, outlook

Due to their specific combination of properties, RO data are particularly well suited for climate monitoring in the atmosphere. Data from the CHAMP mission now cover a period of over 5 years, providing the first opportunity to create continuous multi-year RO climatologies. A period of missing CHAMP data from July 3, 2006 to August 8, 2006 can be bridged with RO data from the GRACE satellite. We have built zonal and seasonal mean (and monthly mean) climatologies for the atmospheric parameters refractivity, pressure, geopotential height and (dry) temperature together with corresponding estimates for the observational and sampling errors based on RO data from the CHAMP satellite. Our results show that accurate zonal mean seasonal climatologies with 10° latitudinal resolution between 4–8 and 30 km altitude can be obtained even with data from a single RO receiver. We compared the CHAMP climatologies with ECMWF derived climatologies and could show that CHAMP data can already now serve as reference for existing state-of-the-art climatologies. The overall agreement between 4–8 and 30 km is in general very good with systematic differences <0.5 K in most parts of the domain. We show that large systematic differences (exceeding 2 K) in the tropical tropopause region and above Antarctica in southern winter can almost entirely be attributed to errors in the ECMWF analyses. The "true" systematic error of CHAMP seasonal and zonal mean climatologies can currently not be determined to a level <0.5 K. It is, however, the dominant contribution to the observational error, since the uncertainty of the mean (statistical error) is <0.1 K almost everywhere. The average CHAMP sampling error for seasonal zonal means in the UTLS is <0.2 K; it is dominated by uneven spatial sampling. The effect of uneven sampling in local time is comparatively negligible. Systematic errors and sampling errors contribute to the total error of CHAMP climatologies, most probably in about equal proportion. If the systematic error is indeed near 0.1 K, i.e., approaching the theoretical potential of the RO measurement principle, the total error is dominated by the sampling component. Overall, the results suggest that the total error of this new type of UTLS temperature climatologies is <0.5 K between 4–8 and 30 km.

The data provide a valuable basis for climate monitoring, given the expected long-term stability of RO data. Already now RO based climatologies have the potential to improve modern operational climatologies in regions where the data coverage and/or the vertical resolution and accuracy of RO data is superior to traditional data sources (e.g., high southern latitudes, tropical tropopause region). Our results provide a valuable starting point for RO based climatologies. The recently (April 2006) launched Taiwan/U.S. FORMOSAT-3/COSMIC constellation with 6 LEOs started to provide up to ∼2500 RO profiles per day and the MetOp satellite (launched October 2006) will soon provide ∼500 additional daily profiles, allowing for climate monitoring with high accuracy and small residual sampling errors during the coming years.

The CHAMP climatologies will be complemented with data from SAC-C, GRACE, COSMIC, and MetOp in the near feature. The RO climatology data are scheduled to be provided to the community for free access via the data and information center web portal of the WegCenter/UniGraz (http://www.wegcenter.at, >Data&Info Center).

References

Anthes RA, Rocken C, Kuo Y (2000) Applications of COSMIC to meteorology and climate. Terr Atmos Oceanic Sci 11(1):115–156

Beyerle G, Schmidt T, Michalak G, Heise S, Wickert J, Reigber C (2005) GPS radio occultation with GRACE: atmospheric profiling utilizing the zero difference technique. Geophys Res Lett 32:L13806. doi:10.1029/2005GL023109

Beyerle G, Heise S, Kaschenz J, König-Langlo G, Reigber C, Schmidt T, Wickert J (2006) Refractivity biases in GNSS occultation data. In: Foelsche et al. (2006b), pp 37–43. doi:10.1007/3-540-34121-8_4

Borsche M, Gobiet A, Steiner AK, Foelsche U, Kirchengast G, Schmidt T, Wickert J (2006) Pre-operational retrieval of radio occultation based climatologies. In: Foelsche et al. (2006b) pp 315–324. doi:10.1007/3-540-34121-8_26

Borsche M, Kirchengast G, Foelsche U (2007), Tropical tropopause climatology as observed with radio occultation measurements from CHAMP compared to ECMWF and NCEP analyses. Geophys Res Lett 34:L03702. doi:10.1029/2006GL027918

Christy JR, Spencer RW (2003) Reliability of satellite data sets. Science 301:1046–1047

European Centre for Medium-Range Weather Forecasts (ECMWF) (2003) Changes to the operational forecasting system. ECMWF Newslett 99:1–2

European Centre for Medium-Range Weather Forecasts (ECMWF) (2004) IFS Documentation CY28rl, Reading

European Centre for Medium-Range Weather Forecasts (ECMWF) (2005) Changes to the operational forecasting system. ECMWF Newslett 106:1–2

Fjeldbo G, Kliore AJ, Eshleman VR (1971) The neutral atmosphere of Venus as studied with the Mariner V radio occultation experiments. Astron J 76:123–140

Foelsche U, Kirchengast G (2004) Sensitivity of GNSS radio occultation data to horizontal variability in the troposphere. Phys Chem Earth 29(2–3):225–240. doi:10.1016/j.pce.2004.01.007

Foelsche U, Kirchengast G, Steiner AK (2003) Global climate monitoring based on CHAMP/GPS radio occultation data. In: Reigber C, Lühr H, Schwintzer P (eds) First CHAMP mission results for gravity, magn., atm. Studies. Springer, Heidelberg, pp 397–407

Foelsche U, Gobiet A, Loescher A, Kirchengast G, Steiner AK, Wickert J, Schmidt T (2005) The CHAMPCLIM project: an overview. In: Reigber C, Luehr H, Schwintzer P, Wickert J (eds) Earth observation with CHAMP: Results from three years in orbit. Springer, Heidelberg, pp 615–619. doi:10.1007/3-540-26800-6_98

Foelsche U, Borsche M, Steiner AK, Pirscher B, Lackner BC, Gobiet A, Kirchengast G (2006a) CHAMP radio occultation based climatologies for global monitoring of climate change. Weg-Center Rep for FFG-ALR 3/2006, 52 pp, http://www.wegcenter.at (>Research>ARSCliSys>Publications)

Foelsche U, Kirchengast G, Steiner AK (eds) (2006b) Atmosphere and climate: studies by occultation methods. Springer, Heidelberg, 336 pp. doi:10.1007/3-540-34121-8

Foelsche U, Gobiet A, Steiner AK, Kirchengast G, Borsche M, Schmidt T, Wickert J (2006c) Global climatologies based on radio occultation data: The CHAMPCLIM project. In: Foelsche et al. (2006b), pp 303–314. doi:10.1007/3-540-34121-8_25

GCOS (2004) Global climate observing system implementation plan for the global observing system for climate in support of UNFCCC. WMO-TD 1219, WMO, Geneva, 136 pp

Gobiet A, Kirchengast G (2004) Advancements of GNSS radio occultation retrieval in the upper stratosphere for optimal climate monitoring utility. J Geophys Res 109:D24110. doi:10.1029/2004JD005117

Gobiet A, Steiner AK, Retscher C, Foelsche U, Kirchengast G (2004) Radio occultation data and algorithms validation based on CHAMP/GPS data. IGAM/UniGraz Tech Rep for ASA 1/2004, 46 pp

Gobiet A, Kirchengast G, Wickert J, Retscher C, Wang D-Y, Hauchecorne A (2005a) Evaluation of stratospheric radio occultation retrieval using data from CHAMP, MIPAS, GOMOS, and ECMWF analysis fields. In: Reigber C et al (eds) Earth observation with CHAMP—results from three years in orbit. Springer, Berlin, pp 531–536. doi:10.1007/3-540-26800-6_84

Gobiet A, Foelsche U, Steiner AK, Borsche M, Kirchengast G, Wickert J (2005b) Climatological validation of stratospheric temperatures in ECMWF operational analyses with CHAMP radio occultation data. Geophys Res Lett 32:L12806. doi:10.1029/2005GL022617

Gobiet A, Kirchengast G, Manney GL, Borsche M, Retscher C, Stiller G (2007) Retrieval of temperature profiles from CHAMP for climate monitoring: intercomparison with Envisat MIPAS and GOMOS and different atmospheric analyses. Atmos Chem Phys 7:3519–3536

Gorbunov ME (2002) Canonical transform method for processing radio occultation data in the lower troposphere. Radio Sci 37:1076. doi:10.1029/2000RS002592

Hajj GA, Ao CO, Iijima PA, Kuang D, Kursinski ER, Mannucci AJ, Meehan TK, Romans LJ, de la Torre Juarez M, Yunck TP (2004) CHAMP and SAC-C atmospheric occultation results and inter-comparisons. J Geophys Res 109:D06109. doi:10.1029/2003JD003909

Healy SB (2001a) Radio occultation bending angle and impact parameter errors caused by horizontal refractive index gradients in the troposphere: a simulation study. J Geophys Res 106(D11):11875–11889

Healy SB (2001b) Smoothing radio occultation bending angles above 40 km. Ann Geophys 19:459–468

Healy SB (2006) Operational assimilation of GPS radio occultation measurements at ECMWF. ECMWF Newslett 111:6–11

Healy SB, Thépaut J-N (2006) Assimilation experiments with CHAMP GPS radio occultation measurements, QJR Meteorol Soc 132:605–623

IPCC (2001) Climate change 2001: The scientific basis. Cambridge University Press, Cambridge, 881 pp

Jensen AS, Lohmann M, Benzon HH, Nielsen A (2003) Full spectrum inversion of radio occultation signals. Radio Sci 38:1040. doi:10.1029/2002RS002763

Kirk-Davidoff DB, Goody RM, Anderson JG (2004) Analysis of sampling errors for climate monitoring satellites. J Clim 18:810–822

König R, Zhu S, Reigber C, Neumayer KH, Meixner H, Galas R, Baustert G, Schwintzer P (2002) CHAMP rapid orbit

determination for GPS atmospheric limb sounding. Adv Space Res 30(2):289–293

Kursinski ER, Hajj GA, Schofield JT, Linfield RP, Hardy KR (1997) Observing Earth's atmosphere with radio occultation measurements using the Global Positioning System. J Geophys Res 102:23429–23465

Mears CA, Wentz FJ (2005) The effect of diurnal correction on satellite-derived lower tropospheric temperature. Science 309:1548–1551. doi:10.1126/science.1114772

Leroy SS (1997) The measurement of geopotential heights by GPS radio occultation. J Geophys Res 102(D6):6971–6986

Leroy SS, Dykema JA, Anderson JG (2006) Climate benchmarking using GNSS occultation. In: Foelsche et al. (2006b) pp 287–301. doi:10.1007/3-540-34121-8_24

Loiselet M, Stricker N, Menard Y, Luntama J-P (2000) GRAS—MetOp's GPS-based atmospheric sounder. ESA Bull 102:38–44

Pirscher B, Foelsche U, Lackner BC, Kirchengast G (2007) Local time influence in single-satellite radio occultation climatologies from Sun-synchronous and non-Sun-synchronous satellites. J Geophys Res 112:D11119. doi:10.1029/2006JD007934

Ramaswamy V, Chanin ML, Angell J, Barnett J, Gaffen D, Gelman M, Keckhut P, Koshelkov Y, Labitzke K, Lin JJR, O'Neill A, Nash J, Randel W, Rood R, Shine K, Shiotani M, Swinbank R (1999) Stratospheric temperature trends: observations and model simulations. Rev Geophys 19:71–122

Rieder MJ, Kirchengast G (2001), Error analysis and characterization of atmospheric profiles retrieved from GNSS occultation data. J Geophys Res 106:31755–31770

Rocken C, Anthes R, Exner M, Hunt D, Sokolovskiy S, Ware R, Gorbunov M, Schreiner W, Feng D, Herman B, Kuo YH, Zou X (1997) Analysis and validation of GPS/MET data in the neutral atmosphere. J Geophys Res 102:29849–29866

Rocken C, Kuo Y, Schreiner WS, Hunt D, Sokolovskij S, McCormick C (2000) COSMIC system description. Terr Atmos Ocean Sci 11:21–52

Schmidt T, Heise S, Wickert J, Beyerle G, Reigber C (2005) GPS radio occultation with CHAMP and SAC-C: global monitoring of thermal tropopause parameters. Atmos Chem Phys 5:1473–1488

Schmidt T, Beyerle G, Heise S, Wickert J, Rothacher M (2006) A climatology of multiple tropopauses derived from GPS radio occultations with CHAMP and SAC-C. Geophys Res Let 33:L04808. doi:10.1029/2005GL024600

Schroeder T, Leroy S, Stendel M, Kaas E (2003) Validating the microwave sounding unit stratospheric record using GPS occultation. Geophys Res Lett 30:1734. doi:10.1029/2003GL017588

Seidel DJ, Angell JK, Christy J, Free M, Klein SA, Lanzante JR, Mears C, Parker D, Schabel M, Spencer R, Sterin A, Thorne P, Wentz F (2004), Uncertainty in signals of large-scale variations in radiosonde and satellite upper-air temperature trends. J Clim 17(11):2225–2240

Sherwood SC, Lanzante JR, Meyer CL (2005) Radiosonde daytime biases and late-20th century warming. Science 309:1556–1559. doi:10.1126/science.1115640

Smith EK, Weintraub S (1953) The constants in the equation for atmospheric refractive index at radio frequencies. Proc IRE 41:1035–1037

Sokolovskiy SV (2003), Effect of superrefraction on inversions of radio occultation signals in the lower troposphere. Radio Sci 38(3):1058. doi:96810.1029/2002RS002728

Steiner AK, Kirchengast G (2005) Error analysis for GNSS radio occultation data based on ensembles of profiles from end-to-end simulations. J Geophys Res 110:D15307. doi:10.1029/2004JD005251

Steiner AK, Kirchengast G, Ladreiter HP (1999) Inversion, error analysis, and validation of GPS/MET occultation data. Ann Geophys 17:122–138

Steiner AK, Kirchengast G, Foelsche U, Kornblueh L, Manzini E, Bengtsson L (2001) GNSS occultation sounding for climate monitoring. Phys Chem Earth A 26:113–124

Steiner AK, Löscher A, Kirchengast G (2006) Error characteristics of refractivity profiles retrieved from CHAMP radio occultation data. In: Foelsche et al. (2006b), pp 27–36. doi:10.1007/3-540-34121-8_3

Syndergaard S (1999) Retrieval analysis and methodologies in atmospheric limb sounding using the GNSS radio occultation technique. DMI Sci Rep 99–6, Danish Met Inst, Copenhagen, 131 pp

Vedel H, Stendel M (2003) On the direct use of GNSS refractivity measurements for climate monitoring. In: Stauning P et al (eds) Proc 4'th Oersted Intern Science Team Conf (OIST-4). Danish Met Inst, Copenhagen, pp 275–278

Vinnikov KY, Grody NC (2003) Global warming trend of mean tropospheric temperature observed by satellites. Science 302:269–272

Vorob'ev VV, Krasil'nikova TG (1994) Estimation of the accuracy of the atmospheric refractive index recovery from Doppler shift measurements at frequencies used in the NAVSTAR system. Phys Atmos Ocean 29:602–609

Wickert J, Reigber C, Beyerle G, König R, Marquardt C, Schmidt T, Grunwaldt L, Galas R, Meehan T, Melbourne W, Hocke K (2001) Atmosphere sounding by GPS radio occultation: first results from CHAMP. Geoph Res Lett 28:3263–3266

Wickert J, Schmidt T, Beyerle G, König R, Reigber C, Jakowski N (2004) The radio occultation experiment aboard CHAMP: operational data analysis and validation of vertical atmospheric profiles. J Met Soc Japan 82:381–395

Wickert J, Beyerle G, König R, Heise S, Grunwaldt L, Michalak G, Reigber C, Schmidt T (2005) GPS radio occultation with CHAMP and GRACE: a first look at a new and promising satellite configuration for global atmospheric sounding. Ann Geophys 23:653–658

Wu B-H, Chu V, Chen P, King T (2005) FORMOSAT-3/COSMIC science mission update. GPS Solut 9:111–121. doi:10.1007/s10291-005-0140-z

Yuan LL, Anthes RA, Ware RH, Rocken C, Bonner WD, Bevis MG, Businger S (1993) Sensing climate change using the Global Positioning System. J Geophys Res 98:14925–14937

Yunck TP, Liu CH, Ware R (2000) A history of GPS sounding. Terrestr Atmos Ocean Sci 11:1–20